Geophysical Research Letters

RESEARCH LETTER
10.1029/2024GL111544

Special Collection:
Integrating In Situ, Remote Sensing, And Physically Based Modeling Approaches to Understand Global Freshwater Ice Dynamics

Influence of Atmospheric Rivers on Alaskan River Ice

Russ Limber[1,2], Elias C. Massoud[2], Bin Guan[3,4], Forrest M. Hoffman[2], and Jitendra Kumar[2]

[1]The University of Tennessee, Knoxville, Knoxville, TN, USA, [2]Oak Ridge National Laboratory, Oak Ridge, TN, USA, [3]Joint Institute for Regional Earth System Science and Engineering, University of California, Los Angeles, CA, USA, [4]Jet Propulsion Laboratory, California Institute of Technology, Pasadena, CA, USA

Abstract Atmospheric rivers (ARs) transport vast amounts of moisture from low to high latitude regions. One region particularly impacted by ARs is Interior Alaska (AK). We analyze the impact of ARs on the annual river ice breakup date for 26 locations in AK. We investigate the AR-driven rise in local air temperatures and explore the relationship between ARs and precipitation, including extremes and interannual variability. We found that AR events lead to an increase in local air temperatures for over 1 week (by ≈1 °C). ARs account for 40% of total precipitation, explain 47% of precipitation variability, and make up 59% of extreme precipitation events, each year. By estimating the heat transfer between winter precipitation and the river ice surface, we conclude that increased precipitation during the coldest period of the year delays river ice breakup dates, while precipitation occurring close to the breakup date has little impact on breakup timing.

Plain Language Summary Atmospheric rivers (ARs) are large storm systems originating in tropical and mid-latitude regions capable of depositing large amounts of precipitation in high latitude regions. Using river ice breakup data throughout Interior Alaska (AK) we set out to explore the relationship between ARs and annual river ice breakup timing from 1980 to 2023. We found that daily air temperature increases can last up to 13 days after an AR event. ARs account for 40% of total precipitation, explain 47% of the variability of precipitation, and make up 59% of extreme precipitation events, on average annually. Using the mass and temperature of precipitation accumulated on the river ice surface, we approximated thermal energy exchange between precipitation and the river ice surface. The magnitude of energy exchange was then correlated to river ice breakup timing. We found that greater amounts of precipitation from both AR and non-AR induced precipitation, occurring relatively close to river ice breakup dates have little correlation to the breakup date. However, increased precipitation during the coldest period of the year (typically late December to early February) is strongly inversely correlated with river ice breakup timing and seems to delay the breakup date.

Key Points:

- Atmospheric rivers (ARs) can lead to over a week-long persistent increase in dailyair temperatures over Interior Alaska (AK)
- In AK, ARs account for 40% of annual precipitation, 59% of extreme precipitation and explain 47% of interannual variability of precipitation
- Precipitation during the coldest months delays the annual breakup date of river ice, precipitation close to the breakup date has less impact

Supporting Information:

Supporting Information may be found in the online version of this article.

Correspondence to:

R. Limber,
Limberr62@ornl.gov

Citation:

Limber, R., Massoud, E. C., Guan, B., Hoffman, F. M., & Kumar, J. (2024). Influence of atmospheric rivers on Alaskan river ice. *Geophysical Research Letters*, *51*, e2024GL111544. https://doi.org/10.1029/2024GL111544

Received 25 JUL 2024
Accepted 20 NOV 2024

1. Introduction

Atmospheric rivers (ARs) are narrow corridors of intense water vapor that significantly influence hydrologic events, transporting water vapor from the Tropics and mid-latitudes (Ralph et al., 2018). It is estimated that ARs are responsible for as much as 90% of poleward water vapor transport at midlatitudes (Zhu & Newell, 1998). ARs contribute to extreme precipitation events across various regions worldwide (Espinoza et al., 2018; Massoud et al., 2019), including Western North America (Dettinger et al., 2004; Neiman et al., 2008; Guan et al., 2010; Paul J., Lawrence J., F. Martin, Mimi, & Gary A., 2011; Ralph et al., 2006; F. Martin et al., 2019; Dettinger et al., 2011) Europe (Harald & Andreas, 2013; Lavers et al., 2013), the Middle East (Esfandiari & Shakiba, 2024; Lashkari & Esfandiari, 2020; Massoud et al., 2020), and Western South America (Viale et al., 2018). In recent years, the impacts of ARs on the cryosphere such as Greenland (Mattingly et al., 2018) and Antarctica (Maclennan et al., 2022a, 2022b; Gorodetskaya et al., 2014; Wille et al., 2021), have been more extensively analyzed. In addition, a growing number of works investigating the relationship between ARs and Arctic regions have been undertaken (Hegyi & Taylor, 2018; Lauer et al., 2023; Li et al., 2022; Ma et al., 2023; Wang et al., 2024; Zhang et al., 2023). Evidence shows that between 1981 and 2020, higher atmospheric moisture content was significantly correlated with lower sea ice coverage over almost the entire Arctic Ocean (Li et al., 2022). For those same years, another analysis found that 100% of extreme temperature events in the Arctic (above 0 °C) coincide with the presence of ARs (Ma et al., 2023). Analyses have noted a relationship between frequent AR activity and sea ice loss, caused by increased rainfall (Hegyi & Taylor, 2018; Li et al., 2022; Zhang et al., 2023). However, Arctic systems are complicated, as the intense moisture transport within ARs can also result in heavy snowfall events, thus contributing to the accumulation of snowpack, especially in mountainous

regions (Guan et al., 2010; Saavedra et al., 2020). Under the right conditions, this relationship has been found to actually increase the mass balance of glaciers (Bravo et al., 2024). Little et al. (2019) found ARs to be the primary drivers of both highest ablation and snowfall events, substantially impacting glacier mass balance at Brewster Glacier in New Zealand. Understanding the role of ARs in the cryosphere is essential for assessing their broader impact on regional water resources and glacier dynamics in a changing climate.

While a number of works have explored the relationship between ARs and sea ice, glaciers, and ice sheets, to our knowledge there has been no study that investigates the relationship between ARs and Arctic river ice. Past works have investigated the climatological drivers of river ice breakup to include three main, potential drivers: hydraulic, mechanical and thermodynamic processes (T. Prowse, Bonsal, Duguay, & Lacroix, 2007). Paily et al. identified the surface heat exchange between the river ice surface and the air as a vital component of a comprehensive river ice breakup model (Paily et al., 1974). This concept was expanded upon when other deterministic river ice breakup models were proposed (G. Ashton, 1986; Jasek, 1998; Shen, 2010). Through such analyses, it is recognized that an increase in precipitation leads to an increase in streamflow, altering the hydraulics associated with river ice breakup, and potentially accelerating mechanical breakup events (G. Ashton, 1986). It has also been proposed that increased snow pack as a result of increased precipitation contributes to breakup severity (T. D. Prowse & Beltaos, 2002). Using breakup records throughout Interior Alaska (AK) from the Alaska-Pacific River Forecast Center Database (the same breakup records used in this analysis which also includes locations in Western Canada) Bieniek et al. (2011) determined that winter precipitation plays a relatively minor role in impacting the breakup timing of river ice and if anything accelerates the breakup timing as a result of increased streamflow. They also report that increased storm activity in the spring leads to increased surface air temperature, leading to earlier breakup dates (Bieniek et al., 2011). However, their analysis used only 4 sites (as opposed to the 26 used in this analysis) and aggregated precipitation seasonally, without accounting for the interaction between winter precipitation and temperature that occurs at a finer temporal resolution. The current study focuses on the thermodynamic effect of large scale AR processes on river ice break up.

Our analysis aims to answer the following questions: (a) Since ARs have been known to impact Arctic systems by increasing temperatures, is there a change in air temperature in different regions of AK corresponding to the presence of ARs? (b) How do ARs contribute to precipitation throughout AK, considering how ARs impact total annual precipitation, interannual variability, and extreme events? (c) How do ARs impact the timing of river ice breakup, does the presence of ARs accelerate or delay the timing of river ice breakup? Are ARs unique to other forms of precipitation in this regard?

2. Data

2.1. Atmospheric Rivers Database

Similar to previous studies, we define ARs using integrated vapor transport (IVT) from the fifth generation European Center for Medium-Range Weather Forecasts Reanalysis (ERA5) (Hersbach et al., 2023). AR detection is based on version four of the tARget algorithm (Guan, 2024; Guan & Waliser, 2024) at the original resolution of ERA5, that is, 0.25° × 0.25°. Originally developed in Guan and Waliser (2015), updated and validated with dropsonde data (Guan et al., 2018), and further updated in (Guan & Waliser, 2019, 2024), this global detection algorithm is based on a combination of IVT magnitude, direction, and geometry characteristics to objectively identify ARs. This algorithm was shown to have over 90% agreement in detecting AR landfall dates when compared with regional AR detection methods for Western North America (Neiman et al., 2008), the United Kingdom (Lavers et al., 2011), and East Antarctica (Gorodetskaya et al., 2014). The latest version of the global AR database (Guan, 2024) based on this algorithm is employed in our study, which includes refinement in polar regions (see details in Guan & Waliser, 2024). A map showing the mean IVT by AR for the year 2021 over AK can be viewed in the supplementray information (Figure S1 in Supporting Information S1). Each point location samples the raster creating a specific time series of AR events at its corresponding closest grid cell (this sampling methodology is true for all raster data used in the analysis). To compare meteorological products and assess potential uncertainties in our results, we also conducted our analysis, applying the detection algorithm to data from the National Center for Environmental Protection (NCEP) Reanalysis data product at its native resolution of 2.5° × 2.5° (Kalnay et al., 1996). For brevity, we focus our results and discussions here onward on higher resolution ERA5 based analysis, however corresponding results from NCEP data based analysis are available in Supporting Information S1.

10.1029/2024GL111544

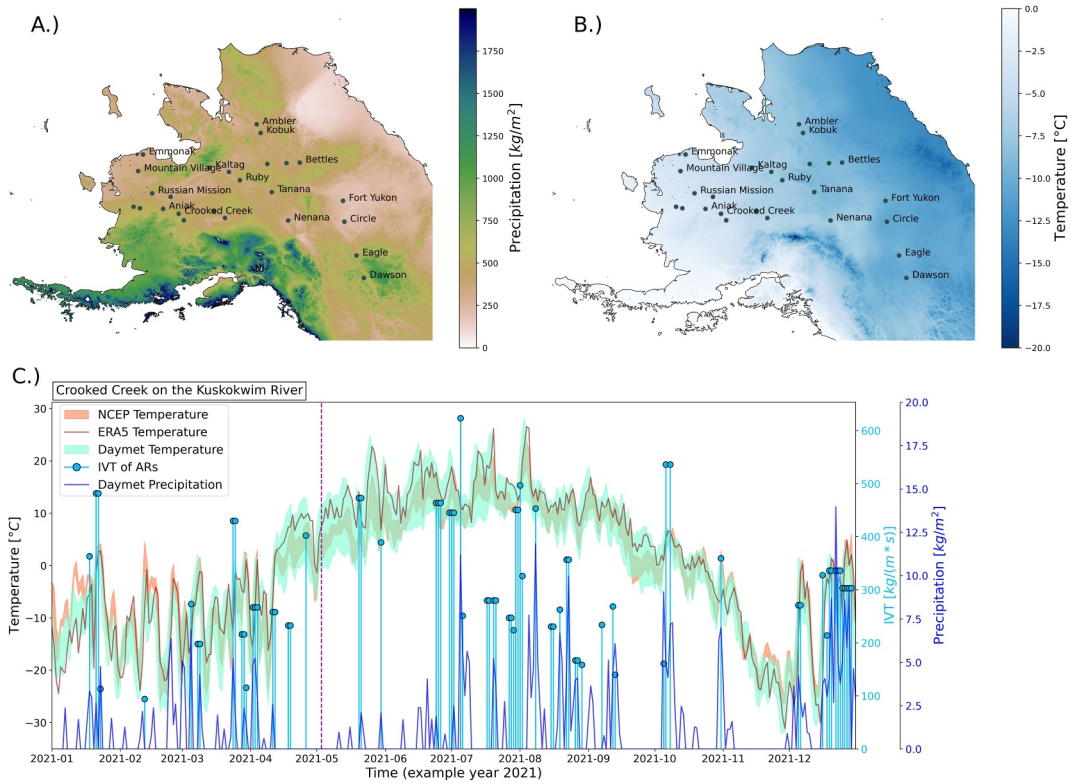

Figure 1. (a) Map showing annual total precipitation for the year 2021 $\left(\frac{\text{kg}}{\text{m}^2}\right)$. (b) Map of average daily temperature for 2021 (°C). (c) One of the 26 locations (Crooked Creek on the Kuskokwim River) for the year 2021. The coral and light green represent the daily temperature profiles (fill plot of $T_{\text{min}} - T_{\text{max}}$) from NCEP (at 1000mb) and Daymet 2m air temperature data, respectively (°C). Maroon line represents the 2 m air temperature for ERA5 (°C). Dark blue line shows precipitation from Daymet $\left(\frac{\text{kg}}{\text{m}^2}\right)$ relative to the secondary axis in dark blue on the right. The light blue stem plots depict the IVT of AR events $\left(\frac{\text{kg}}{\text{m} * \text{s}}\right)$ relative to the secondary axis in light blue on the right. The vertical purple dashed line shows the breakup date for the Kuskokwim River in 2021 at Crooked Creek.

2.2. Daymet Daily Surface Weather and Climatological Summaries

Daily minimum (T_{min}) and maximum (T_{max}) temperatures and precipitation data were obtained from Daymet (M. Thornton et al., 2022). Daymet provides continuous and gridded estimates of daily weather at 1km × 1km resolution. Daymet precipitation, T_{min} and T_{max}, show strong agreement with the ERA5 temperature time series over our region of interest (Figure 1c). Daymet is derived by interpolating and extrapolating from in situ instruments and meteorological stations, and represents a robust data set for precipitation and temperature predictions across North America (P. E. Thornton et al., 2021). This data set has been a standard for validation among several analyses related to Arctic regions (Akinsanola et al., 2024; Diro & Sushama, 2019). Figures 1a and 1b show the annual mean precipitation and temperature for the year 2021 across Alaska. For one of the study locations, Crooked Creek at the Kuskokwim River, Figure 1c shows the time series of precipitation, temperature and AR events for the year 2021.

2.3. River Ice Breakup Observations

Observations for river ice breakup dates were obtained from the Alaska-Pacific River Forecast Center database with locations extending from Western Alaska into Western Canada. While exact coordinates were unavailable, location coordinates were estimated based on proximity to weather stations and airports, to maintain spatial consistency with inputs used in Daymet's meteorological models. We identified 26 locations (shown in Figures 1a and 1b) in the database that had at least 35 breakup records between 1980 and 2023 (the current temporal availability of Daymet), although breakup records go as far back as 1896 for some locations. The 35 breakup

records threshold was used because it allowed for the greatest number of locations with the most complete time series necessary for statistical analysis. There is always one breakup date per year, but not every year had a recorded date, so some years are represented as empty values in the data set. On average, recorded breakup dates range from mid-March to late-June. This data set has been used in several other studies looking at the breakup timing of Alaskan river ice, such as (Bieniek et al., 2011; Brown et al., 2018; Murphy et al., 2022). As an example, the breakup date for Crooked Creek at the Kuskokwim River in 2021 occurred in early May and is depicted in Figure 1c with a vertical purple dashed line.

3. Methods

To assess the influence of ARs on local temperature, we analyze the relationship between the presence of an AR and the temperature change at a specific location. The presence of an AR is represented numerically as a binary value indicating whether or not an AR is active on a particular date. We then estimate how many days this change in temperature persists. To do this, we conducted a pairwise *t*-test using a varying temporal window. In other words, for each AR occurrence in the data set, a pre—AR time window and post—AR time window each equal to n days in length was created before and after the AR event date, respectively, whereby: $n \in \{1, 2, 3, \ldots, 14\}$. For values of n greater than one day the mean was calculated within each time window for $T_{\min}$ and $T_{\max}$. These averaged temperatures were then calculated over all locations. Mean temperature pairs were assessed using a one tailed pairwise *t*-test to check whether ARs increased the local temperature over period of time n ($\alpha = 0.05$). For example, if $n = 3$ assessing $T_{\min}$, then the mean of $T_{\min}$ 3 days prior to each AR event will be compared to the mean of $T_{\min}$ for the 3 days post each AR event.

We explored AR contribution to precipitation by separating precipitation events occurring on days with an active AR. We then used the Wilcoxon rank-sum test (Rey & Neuhauser, 2011) to test the hypothesis that AR events tend to produce more precipitation than other precipitation events. We opted to use a non-parametric test (Wilcoxon rank-sum test) because the distributions of precipitation were shown to not be normal after log transformation using the Shapiro-Wilks test (Shapiro & Wilk, 1965). We also estimated the interannual variability of precipitation associated with ARs by conducting a univariate ordinary least squares regression (OLS). For extremes, we extracted the top 5% of precipitation events and determined what fraction of those events occurred on days with an active AR event.

To determine the impact that ARs have on river ice breakup timing, we estimate the heat transfer between the river ice and the precipitation accumulating on the surface. Assuming presence of a frozen layer of ice on the river surface, we estimate the sensible heat transfer between the river surface and incoming precipitation using Equation 1. Latent heat transfer fluxes were assumed to be relatively small and thus ignored in our simplified heat transfer calculations. The specific heat of precipitation in Equation 1 is represented as either liquid water or snow as determined by air temperature. Given that Alaska is at a high latitude with heat transfer calculated between the start of freeze-up (which we conservatively set to be September 15th) to the breakup, it can be assumed that in most cases the precipitation is in the form of snow during the colder half of the year.

$$q_t = \rho \cdot m \cdot \Delta T \tag{1}$$

where q_t is heat flux $\left(\frac{\mathrm{J}}{\mathrm{m}^2}\right)$ at a given day t; ρ the specific heat of the precipitation (assumed to be either water or snow depending on the temperature) $\left(\frac{\mathrm{J}}{\mathrm{kg}\,^\circ\mathrm{C}}\right)$; ΔT is the difference between the temperature of the precipitation which is approximated using $T_{\min}$ as a proxy, and the river ice surface which is assumed to be at 0 °C; m the mass of the precipitation per unit area $\left(\frac{\mathrm{kg}}{\mathrm{m}^2}\right)$. We conducted the analysis using $T_{\min}$ and $T_{\max}$, and found the results to be very similar. We present the results using $T_{\min}$ as a proxy for precipitation temperature, as the results were marginally more consistent across locations.

Heat transfer fluxes were calculated as a daily series for a period of 6 months prior to the breakup date. Time of occurrence and thermal conditions associated with precipitation events during winter and spring have differential impacts to reinforce versus weaken the river ice layer and thus the date of the breakup. We fit a temporal bias function (Equation 2), a double exponential function, applied to the heat transfer equation to assess which days within the 6 months prior to breakup when precipitation events were more impactful on breakup timing. The bias

function is a symmetric unimodal exponential function to help identify the most influential precipitation time period determining the annual time of river ice breakup. This bias function was fit individually for each of the study locations.

$$f(t;\gamma,\kappa,\ DOY,c) = \begin{cases} \dfrac{e^{-\gamma\cdot(-t-DOY)}-1}{\kappa} & \text{if } t < c \\ \dfrac{e^{-\gamma\cdot(t-DOY)}-1}{\kappa} & \text{if } t \geq c \end{cases} \tag{2}$$

where γ is a scale parameter impacting the width of the exponential function; t is time in days; DOY is the Gregorian day of year that the breakup date occurred; c is a location parameter dictating the center placement of the function; κ is a normalizing constant. Finally, Equation 3 solves for $Q_{\text{year, location}}$, the total thermal energy exchange for a given location, for a given breakup year. Equation 3 is tuned over the entire hyperparameter search space for each location and each breakup year, optimized by selecting the parameter values that produce the Pearson correlation coefficient with the greatest absolute value. Here i is the starting day of the time series approximately 6 months prior to the breakup date.

$$Q_{\text{year, location}} = \sum_{t=i}^{t=DOY} f(t;\gamma,\kappa,DOY,c)\cdot q_t \tag{3}$$

4. Results

4.1. Atmospheric Rivers Impact on Temperature

We applied the pairwise t-test comparing pre–AR and post–AR time windows of length n at all locations. Figures 2a and 2b shows the change in p-values for each value of n along with the mean increase in temperature from the pre–AR time window to the post–AR time window for varying time window sizes n. Analysis shows an increase in air temperature during the period following an AR event, with mean temperature increases higher for T_{min} compared to T_{max}, with the difference receding over longer time windows. On average, the temperature differences were statistically significant for T_{min} (based on an $\alpha = 0.05$) for temporal windows up to 13 days after an AR event. For temporal windows up to 10 days, statistical significance was true for all locations within the study as represented by Figure 2a fill plot. The increase in daily minimum temperature can be as high as 1.3 °C ($n = 3$) (Figure 2a). For T_{max}, the differences were statistically significant for up to 8 days after an AR event on average (not including $n = 1$) with an increase as high as 0.67 °C ($n = 4$) (Figure 2b). Statistically significant increases in T_{max} following AR events were true at all locations in our study for $n = \{3\ldots6\}$ as shown in Figure 2b fill plot.

4.2. Atmospheric Rivers Impact on Precipitation

ARs tend to account for 40% of precipitation on average (Figure 2e), with a high degree of variability across years and locations. In 2013 for example, nearly 80% of the total precipitation at some locations occurred on days with active AR events. The results from the Wilcoxon rank-sum test show that precipitation during active ARs tends to be greater in magnitude than non-AR precipitation (test statistic $= -88.30$; p-value ≈ 0.0). In addition, we found that of the top 5% of precipitation events by total rainfall, 59% occurred during active ARs (Figure 2f). Correlating total precipitation from AR days to total annual precipitation using a univariate OLS, we find that the coefficient of determination $\left(R^2\right)$ is equal to 0.47 (Figure 2g). This indicates that precipitation from ARs explains about 47% of the total interannual variability in precipitation, across all 26 locations.

4.3. Transfer of Energy Based on Precipitation

To estimate the impact of precipitation on river ice breakup dates, we use Equation 3 to approximate the heat transfer between precipitation and the river ice surface. Equation 3 was solved using a double exponential bias function to temporally weigh events of higher influence (Figures 3a and 3c), and using uniform weights as a baseline for comparison (Figures 3d and 3f). When using a temporal bias function, the relationship between summated heat transfer due to precipitation and time of river ice breakup were identified with strong correlation

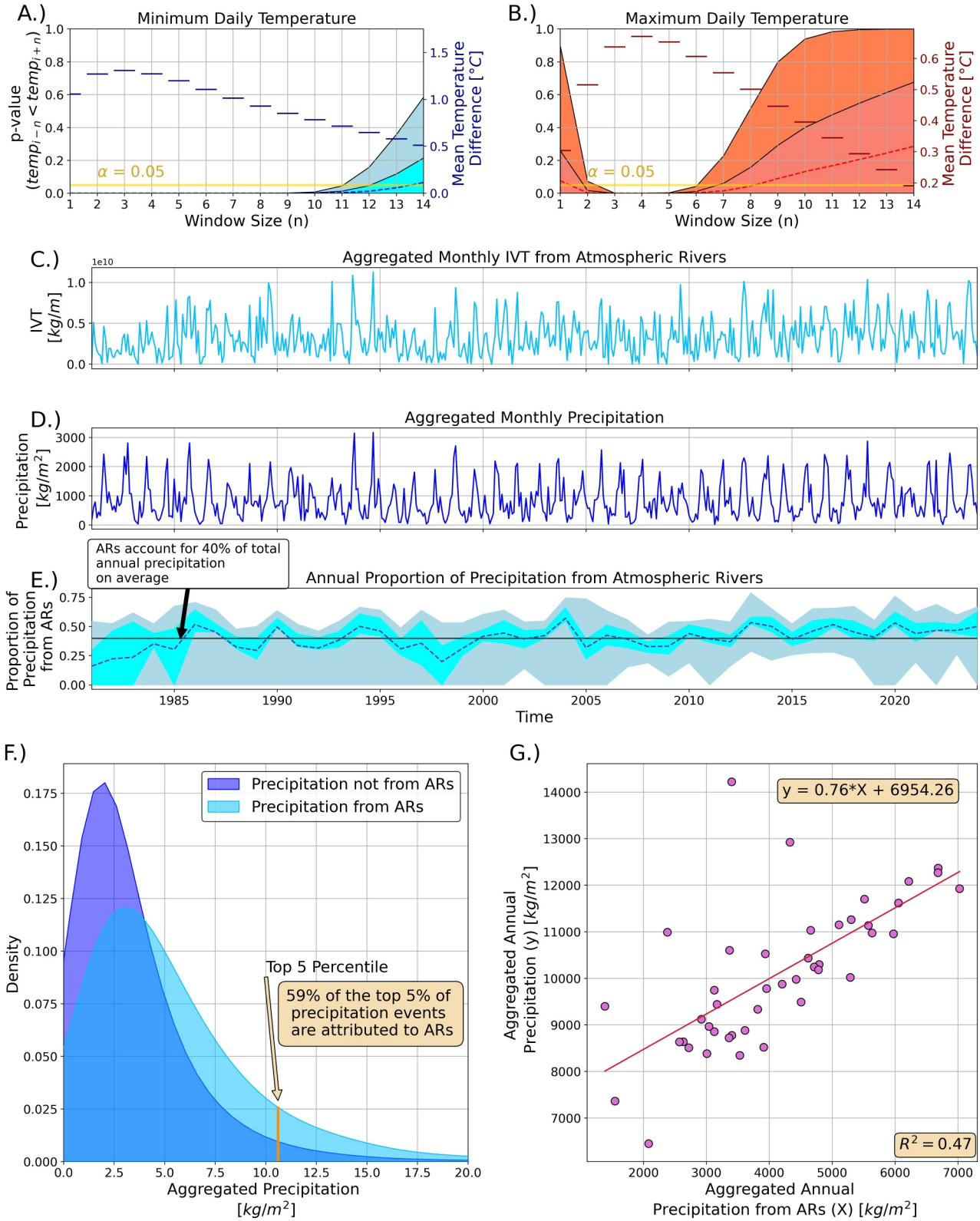

Figure 2.

(Pearson correlation coefficient $(r_p) = -0.82$ and a Spearman correlation coefficient $(r_s) = -0.81$ at Crooked Creek on the Kuskokwim river (Figure 3a). In contrast, very weak correlations were identified when fitting the relationship using temporally uniform weights (Figure 3d), thus highlighting the need for a temporal bias function. We tuned three different cases for Equation 1 whereby the mass of precipitation could be provided by: total precipitation, precipitation from ARs or precipitation not from ARs. This exercise allows us to determine whether or not the aggregated energy accelerates or decelerates the breakup of river ice. We find that there is a strong negative correlation between the heat transfer and the *DOY* on which the river ice breakup occurs (Figure 3a). In this context, negative values along the vertical axis of Figures 3a and 3d are interpreted as a negative heat exchange, suggesting a net cooling effect on the river ice surface as the precipitation below freezing accumulates on the river ice surface. The peak of the temporally weighted bias curve is usually located during the coldest period of the year, typically between late November and early February (Figure 3c). In other words, the presence of high magnitude precipitation events, occurring on colder days of the year show a strong inverse correlation to the time of breakup. For example, referring to Figure 3a, Crooked Creek on the Kuskokwim River has a clear negative trend, whereby the cooling effect of precipitation on the river ice surface delays the *DOY* of the breakup. The frequency of AR events that occurred 6 months prior to the breakup date alone is an insufficient predictor of the breakup date (Figures 3b and 3e).

While Figure 3 focuses on a single selected site, Table S1a in Supporting Information S1, shows the Pearson correlation after tuning parameters c and γ are optimized and applied to Equation 3 individually at each location. The correlation values tend to be high and fairly similar when comparing total precipitation, precipitation from ARs and precipitation not from ARs. This implies that precipitation volume, timing and temperature, influence the breakup timing of river ice, with precipitation from ARs showing little difference to non-AR precipitation. The center of the temporal bias across these categories remains similar with some locations showing variation. In general, the results from the AR detection algorithm using tARget version 4 with ERA5 and the AR detection algorithm using tARget version 3 with NCEP are similar (Tables S1a and S1b in Supporting Information S1).

5. Conclusion and Discussion

This study investigated the impact ARs and non-AR related precipitation events have on 26 river observation points in or close to Interior Alaska. We explored the impact of ARs on local temperature increases throughout the study domain; the contribution of ARs to precipitation events, including variability and extremes; and fused precipitation, temperature and time, with a heat transfer approximation and correlation analysis, to better understand how precipitation events impact river ice breakup timing.

We found that ARs can lead to a persistent increase in $T_{\min}$ by as much as 13 days on average with an increase in temperature as high as 1.3 °C ($n = 3$) (Figure 2a); and 8 days on average (not including $n = 1$) for $T_{\max}$ with an increase in temperature as high as 0.67 °C ($n = 4$) (Figure 2b). We note a small discrepancy when comparing the results from the ERA5 based detection product (Figures 2a and 2b) and the lower resolution NCEP based detection product (Figures S2a and S2b in Supporting Information S1). The NCEP results imply that the statistical significance ($\alpha = 0.05$) persists for 10 days rather than 13 for $T_{\min}$ (Figure S2a in Supporting Information S1). The mean temperature changes are generally similar for both products (Figures 2a and 2b and Figures S2a and S2b in Supporting Information S1). These findings are consistent with many past studies that have shown that warm moisture and an increase in heat flux brought on by ARs can warm the cryosphere (Li et al., 2022; Ma et al., 2023; Wille et al., 2021; Zhang et al., 2023). Our analysis also shows that ARs account for a significant portion of total annual precipitation in Alaska, contributing to 40% of total annual precipitation by volume on

Figure 2. Each subplot uses either the raw or aggregated data from all 26 of the locations used in the analysis (Figures 1a and 1b) (a) and (b) fill plots represent p-values from the paired t-test given time window size n surrounding the AR event date (a $T_{\min}$; (b) $T_{\max}$). Dashed lines inside the fill plots represent the mean, while the filled color curves show interquartile range (25th and 75th percentile). p-values are in relation to the axis on the left side of plots A and (b) Short horizontal lines represent the mean increase in temperature (°C) accompanying each AR, calculated between the pre–AR time window and the post–AR time window. These values are in relation to the color coded secondary axis on the right side of each plot. A gold colored horizontal line showing the level of the t-test equal to 0.05 is shown on each plot. (c) Time series of IVT $\left(\frac{\text{kg}}{\text{m}}\right)$ aggregated monthly. (d) Time series of total precipitation $\left(\frac{\text{kg}}{\text{m}^2}\right)$ aggregated monthly. (e) Proportion of precipitation accounted for by ARs on an annual basis; where light blue depicts the IQR of proportions and blue-gray represents proportions outside of the IQR; the dashed line represents the mean proportion; solid horizontal line represents the global average proportion that is, 0.40. (f) Kernel density plots showing the distribution of local precipitation (dark blue) and precipitation from ARs (light blue). (g) Ordinary least squares regression plot using total annual precipitation from ARs, to predict total annual precipitation $\left(\frac{\text{kg}}{\text{m}^2}\right)$.

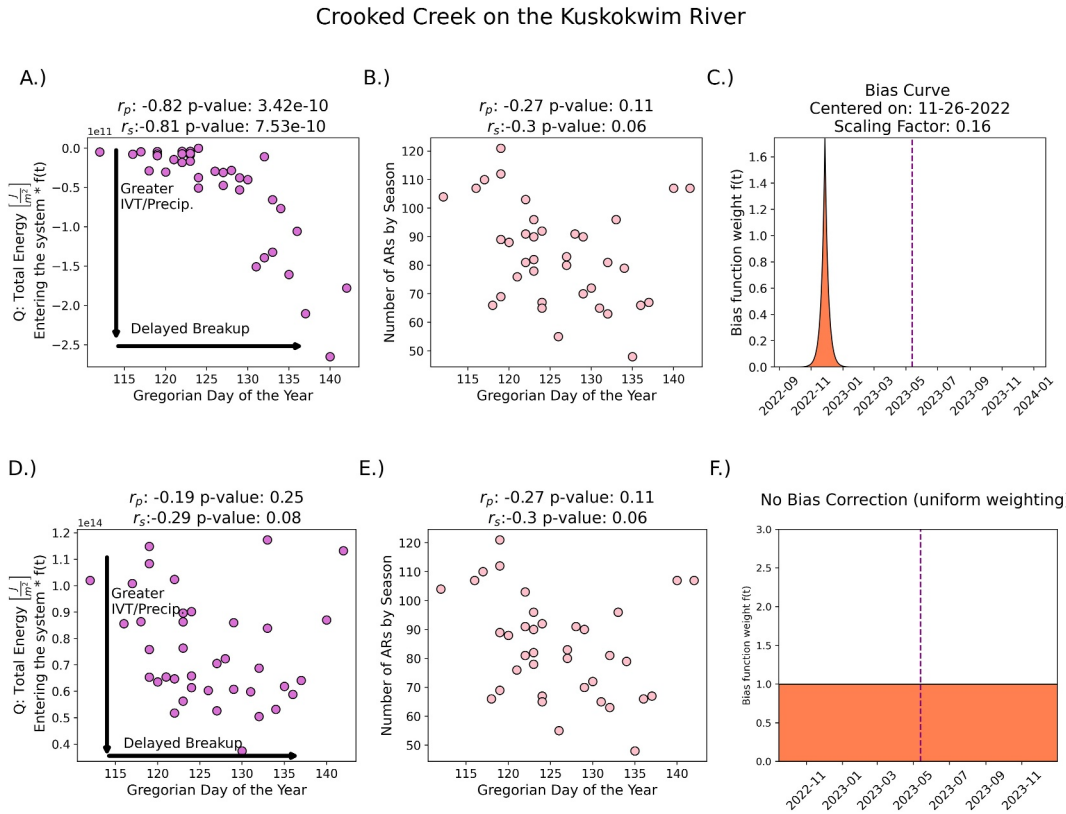

Figure 3. Top row (a) Scatter plot between thermal energy transfer for all precipitation events and *DOY* (the Gregorian day of year that the breakup date occurred). (b) Scatter plot of the number of ARs that occurred in the 6 months prior to the breakup date and *DOY*.(c) Temporal bias curve for the year 2021 with the breakup date represented by the vertical dashed line. bottom row: same as the top row except depicting the results when a temporal bias is not utilized.

average (Figure 2e). ARs also explain 47% of interannual variability (Figure 2g) and lead to 59% of extreme precipitation events (precipitation events within the top 5% of deposition; Figure 2f). These results are consistent with past works, such as Nash et al. (2024) which showed that throughout Southeast Alaska, as few as six annual AR events can account for 68%–91% of precipitation days. Our analysis shows evidence that more frequent and intense precipitation events (including AR events since ARs account for 40% of total precipitation and 59% of extreme precipitation) occurring during the coldest period of the year, appear to delay the annual breakup date of river ice Figure 3a. Our results do not show that ARs are unique relative to non-AR forms of precipitation in this regard, as both appear to delay the breakup date (Table S1a in Supporting Information S1). We discovered no evidence that increased precipitation events of any kind, close to the breakup date, accelerate the breakup date. The delaying of river ice breakup is likely attributed to a combination of heat transfer from precipitation, increased ice accumulation on the river ice surface and structural changes in the river ice as a result of snowfall. Increased snow accumulation increases the albedo of the river surface, as well as provides thermal insulation, mitigating the effects of temperature fluctuations. This is consistent with the extensive analysis conducted by G. D. Ashton (2011), showing that an increase in snow accumulation on the river ice surface for locations across Alaska (many of the same locations used in this analysis) can lead to an increase in river ice thickness, thus reinforcing the river ice structurally. This phenomenon is apparent to a point, at which time the efficacy begins to diminish.

It should be noted that a limitation of our analysis is the assumption that the river ice surface temperature is held constant at 0 °C and that air temperature is a reasonable proxy for the temperature of precipitation. We were unable to find a complete data set on river ice surface temperatures for the locations and time period of our study. Thus, we assume that the mass of liquid, snow, or ice, deposited on the river surface, times its temperature and specific heat, will be sufficient to approximate the heat exchanged in the system. Latent heat was also not accounted for in the analysis. In general, we assume latent heat is relatively small since at high latitudes during the

winter months relatively little phase change is occurring (the temperature rarely goes above freezing). However, it is an important component of the thermodynamic processes surrounding river ice breakup, and we plan to address it in our future work. While our analysis focused on the major thermodynamic drivers of river ice breakup (i.e., temperature, precipitation and time) which are influenced by large scale systems like ARs, the hydrological processes (such as stream flow discharge, temperatures), river morphology and watershed characteristics play an important role in determining the dynamics of the river ice. Incorporating these processes, in addition to AR impacts, would be essential for accurate modeling and prediction of river ice breakup at high latitudes.

Understanding the influence of ARs and other high precipitation events on the timing of river ice breakup in Alaska is crucial for predicting and managing the impacts of climate change in the region, especially since studies have shown that AR frequency and intensity in this region are expected to increase in a warmer world (Espinoza et al., 2018; Massoud et al., 2019). The findings of our analysis suggests that ARs have significant influence on the climate and terrestrial hydrology across Alaska, affecting temperature, precipitation, and in addition to other precipitation events, river ice dynamics. Further research in this area could help improve our understanding of ARs and their role in shaping the climate of high-latitude regions.

Data Availability Statement

Daily meteorological variables used in the analysis (i.e., minimum temperature, maximum temperature and precipitation) were collected from Daymet, via the Oak Ridge National Laboratory, Distributed Active Archive Center for Biogeochemical Dynamics (M. Thornton et al., 2022). River ice breakup records are maintained by the Alaska-Pacific River Forecast Center (Arp et al., 2021). The AR data sets can be accessed via the Global Atmospheric River Dataverse (Guan, 2024). NCEP-NCAR Reanalysis 1 data was obtained from the NOAA Physical Sciences Laboratory, Boulder, Colorado, USA (Kalnay et al., 1996). ERA5 Reanalysis temperature data was obtained from the Copernicus Climate Data Store (Hersbach et al., 2023). All figures were created using matplotlib version 3.5.1 (Caswell et al., 2021; Hunter, 2007), openly available under the Matplotlib license at https://matplotlib.org/. All netcdf files imported from the above sources were operated on using xarray version 2023.1.0 (Hoyer et al., 2023), openly available under the Apache License at https://github.com/pydata/xarray. All of the codes needed to run the analysis and everything required to reproduce this work are available on GitHub at https://github.com/Russtyhub/River_Ice_AR_Analysis.git.

Acknowledgments
This work was supported by the U.S. Department of Energy, Office of Science, Biological and Environmental Research (BER) Regional and Global Model Analysis (RGMA) program, as part of The Interdisciplinary Research for Arctic Coastal Environments (InteRFACE) project. Development of the AR database was supported by NASA and the California Department of Water Resources. This manuscript has been authored in part by UT-Battelle, LLC, under contract DE-AC05-00OR22725 with the US Department of Energy (DOE). The publisher acknowledges the US government license to provide public access under the DOE Public Access Plan (http://energy.gov/downloads/doe-public-access-plan).

References

Akinsanola, A. A., Jung, C., Wang, J., & Kotamarthi, V. R. (2024). Evaluation of precipitation across the contiguous United States, Alaska, and Puerto Rico in multi-decadal convection-permitting simulations. *Scientific Reports*, *14*(1), 1238. https://doi.org/10.1038/s41598-024-51714-3

Arp, C., Bondurant, A., Brown, D., Clement, S., Engram, M., Oxtoby, L., & Spellman, K. (2021). Fresh eyes on river ice in Alaska through remote sensing, field studies, and community-based observations [Dataset]. Retrieved from https://www.weather.gov/aprfc/breakupDB. Accessed on 10 Aug 2024.

Ashton, G. (1986). *River and lake ice engineering*. Water Resources Publications. Retrieved from https://books.google.com/books?id=xglYVjAsnt8C

Ashton, G. D. (2011). River and lake ice thickening, thinning, and snow ice formation. *Cold Regions Science and Technology*, *68*(1), 3–19. https://doi.org/10.1016/j.coldregions.2011.05.004

Bieniek, P. A., Bhatt, U. S., Rundquist, L. A., Lindsey, S. D., Zhang, X., & Thoman, R. L. (2011). Large-scale climate controls of interior Alaska river ice breakup. *Journal of Climate*, *24*(1), 286–297. https://doi.org/10.1175/2010JCLI3809.1

Bravo, C., Cisternas, S., Viale, M., Paredes, P., Bozkurt, D., & García-Lee, N. (2024). Unseasonal atmospheric river drives anomalous glacier accumulation in the ablation season of the subtropical andes. *EGUsphere*, 1–27. https://doi.org/10.5194/egusphere-2024-1958

Brown, D. R. N., Brinkman, T. J., Verbyla, D. L., Brown, C. L., Cold, H. S., & Hollingsworth, T. N. (2018). Changing river ice seasonality and impacts on interior alaskan communities. *Weather, Climate, and Society*, *10*(4), 625–640. https://doi.org/10.1175/WCAS-D-17-0101.1

Caswell, T., Droettboom, M., Lee, A., De Andrade, E., Hoffmann, T., Hunter, J., et al. (2021). matplotlib/matplotlib [Software]. *Zenodo*. Retrieved from https://pypi.org/project/matplotlib/3.5.1/

Dettinger, M. D., Cayan, D. R., Meyer, M. K., & Jeton, A. E. (2004). Simulated hydrologic responses to climate variations and change in the merced, carson, and american river basins, sierra Nevada, California, 1900–2099. *Climatic Change*, *62*(1), 283–317. https://doi.org/10.1023/B:CLIM.0000013683.13346.4f

Dettinger, M. D., Ralph, F. M., Das, T., Neiman, P. J., & Cayan, D. R. (2011). Atmospheric rivers, floods and the water resources of California. *Water*, *3*(2), 445–478. https://doi.org/10.3390/w3020445

Diro, G. T., & Sushama, L. (2019). Simulating canadian arctic climate at convection-permitting resolution. *Atmosphere*, *10*(8), 430. https://doi.org/10.3390/atmos10080430

Esfandiari, N., & Shakiba, A. (2024). The extraordinary atmospheric rivers analysis over the middle east: Large-scale drivers, structure, effective sources, and precipitation characterization. *Dynamics of Atmospheres and Oceans*, *105*, 101430. https://doi.org/10.1016/j.dynatmoce.2023.101430

Espinoza, V., Waliser, D. E., Guan, B., Lavers, D. A., & Ralph, F. M. (2018). Global analysis of climate change projection effects on atmospheric rivers. *Geophysical Research Letters*, *45*(9), 4299–4308. https://doi.org/10.1029/2017GL076968

Gorodetskaya, I. V., Tsukernik, M., Claes, K., Ralph, M. F., Neff, W. D., & Van Lipzig, N. P. M. (2014). The role of atmospheric rivers in anomalous snow accumulation in east Antarctica. *Geophysical Research Letters*, *41*(17), 6199–6206. https://doi.org/10.1002/2014GL060881

Guan, B. (2024). [Code] tracking atmospheric rivers globally as elongated targets (tARget), version 4. [Dataset]. *UCLA Dataverse*. (Accessed on 01-Oct-2024) https://doi.org/10.25346/S6/SF4AFW

Guan, B., Molotch, N. P., Waliser, D. E., Fetzer, E. J., & Neiman, P. J. (2010). Extreme snowfall events linked to atmospheric rivers and surface air temperature via satellite measurements. *Geophysical Research Letters*, *37*(20). https://doi.org/10.1029/2010GL044696

Guan, B., & Waliser, D. (2019). Tracking atmospheric rivers globally: Spatial distributions and temporal evolution of life cycle characteristics. *Journal of Geophysical Research: Atmospheres*, *124*(23), 12523–12552. https://doi.org/10.1029/2019JD031205

Guan, B., & Waliser, D. E. (2015). Detection of atmospheric rivers: Evaluation and application of an algorithm for global studies. *Journal of Geophysical Research: Atmospheres*, *120*(24), 12514–12535. https://doi.org/10.1002/2015JD024257

Guan, B., & Waliser, D. E. (2024). A regionally refined quarter-degree global atmospheric rivers database based on era5. *Scientific Data*, *11*(1), 440. https://doi.org/10.1038/s41597-024-03258-4

Guan, B., Waliser, D. E., & Ralph, F. M. (2018). An intercomparison between reanalysis and dropsonde observations of the total water vapor transport in individual atmospheric rivers. *Journal of Hydrometeorology*, *19*(2), 321–337. https://doi.org/10.1175/JHM-D-17-0114.1

Harald, S., & Andreas, S. (2013). Moisture origin and meridional transport in atmospheric rivers and their association with multiple cyclones. *Monthly Weather Review*, *141*(8), 2850–2868. https://doi.org/10.1175/MWR-D-12-00256.1

Hegyi, B. M., & Taylor, P. C. (2018). The unprecedented 2016–2017 arctic sea ice growth season: The crucial role of atmospheric rivers and longwave fluxes. *Geophysical Research Letters*, *45*(10), 5204–5212. https://doi.org/10.1029/2017GL076717

Hersbach, H., Bell, B., Berrisford, P., Biavati, G., Horányi, A., Muñoz Sabater, J., et al. (2023). ERA5 hourly data on single levels from 1940 to present. Copernicus Climate Change Service (C3S). *Climate Data Store (CDS)* [Dataset]. https://doi.org/10.24381/cds.adbb2d47

Hoyer, S., Roos, M., Joseph, H., Magin, J., Cherian, D., Fitzgerald, C., et al. (2023). xarray [Software]. *Zenodo*. https://doi.org/10.5281/zenodo.7548990

Hunter, J. D. (2007). Matplotlib: A 2d graphics environment [Software]. *Computing in Science & Engineering*, *9*(3), 90–95. https://doi.org/10.1109/MCSE.2007.55

Jasek, M. (1998). 1998 break-up and flood on the yukon river at dawson – Did el niño and climate change play a role? In H. Shen (Ed.), *Ice in surface waters: Proceedings of the 14th international symposium on ice* (pp. 761–768). A.A. Balkema.

Kalnay, E., Kanamitsu, M., Kistler, R., Collins, W., Deaven, D., Gandin, L., et al. (1996). The ncep/ncar 40-year reanalysis project [Dataset]. *Bulletin of the American Meteorological Society*, *77*(3), 437–472. https://doi.org/10.1175/1520-0477(1996)077<0437:TNYRP>2.0.CO;2. Accessed on 01 Oct 2024.

Lashkari, H., & Esfandiari, N. (2020). 05). Identifying atmospheric river events and their paths into Iran. *Theoretical and Applied Climatology*, *140*(3–4), 1125–1137. https://doi.org/10.1007/s00704-020-03148-w

Lauer, M., Rinke, A., Gorodetskaya, I., Sprenger, M., Mech, M., & Crewell, S. (2023). Influence of atmospheric rivers and associated weather systems on precipitation in the arctic. *Atmospheric Chemistry and Physics*, *23*(15), 8705–8726. https://doi.org/10.5194/acp-23-8705-2023

Lavers, D. A., Allan, R. P., Villarini, G., Lloyd-Hughes, B., Brayshaw, D. J., & Wade, A. J. (2013). Future changes in atmospheric rivers and their implications for winter flooding in britain. *Environmental Research Letters*, *8*(3), 034010. https://doi.org/10.1088/1748-9326/8/3/034010

Lavers, D. A., Allan, R. P., Wood, E. F., Villarini, G., Brayshaw, D. J., & Wade, A. J. (2011). Winter floods in britain are connected to atmospheric rivers. *Geophysical Research Letters*, *38*(23). https://doi.org/10.1029/2011GL049783

Li, L., Cannon, F., Mazloff, M. R., Subramanian, A. C., Wilson, A. M., & Ralph, F. M. (2022). Impact of atmospheric rivers on arctic sea ice variations. *EGUsphere*, *2022*, 1–21. Retrieved from https://egusphere.copernicus.org/preprints/2022/egusphere-2022-36/doi:10.5194/egusphere-2022-36

Little, K., Kingston, D. G., Cullen, N. J., & Gibson, P. B. (2019). The role of atmospheric rivers for extreme ablation and snowfall events in the southern alps of New Zealand. *Geophysical Research Letters*, *46*(5), 2761–2771. https://doi.org/10.1029/2018GL081669

Ma, W., Wang, H., Chen, G., Qian, Y., Baxter, I., Huo, Y., & Seefeldt, M. W. (2023). Wintertime extreme warming events in the high arctic: Characteristics, drivers, trends, and the role of atmospheric rivers. *EGUsphere*. https://doi.org/10.5194/egusphere-2023-2018

Maclennan, M. L., Lenaerts, J. T. M., Shields, C., & Wille, J. D. (2022a). Contribution of atmospheric rivers to antarctic precipitation. *Geophysical Research Letters*, *49*(18), e2022GL100585. https://doi.org/10.1029/2022GL100585

Maclennan, M. L., Lenaerts, J. T. M., Shields, C., & Wille, J. D. (2022b). Contribution of atmospheric rivers to antarctic precipitation. *Geophysical Research Letters*, *49*(18). https://doi.org/10.1029/2022GL100585

Martin, R., Jonathan, J. R., Jason, M. C., Michael, D., Michael, A., David, R., et al. (2019). A scale to characterize the strength and impacts of atmospheric rivers. *Bulletin of the American Meteorological Society*, *100*(2), 269–289. https://doi.org/10.1175/BAMS-D-18-0023.1

Massoud, E., Espinoza, V., Guan, B., & Waliser, D. (2019). Global climate model ensemble approaches for future projections of atmospheric rivers. *Earth's Future*, *7*(10), 1136–1151. https://doi.org/10.1029/2019EF001249

Massoud, E., Massoud, T., Guan, B., Sengupta, A., Espinoza, V., De Luna, M., et al. (2020). Atmospheric rivers and precipitation in the middle east and north africa (mena). *Water*, *12*(10), 2863. https://doi.org/10.3390/w12102863

Mattingly, K. S., Mote, T. L., & Fettweis, X. (2018). Atmospheric river impacts on Greenland ice sheet surface mass balance. *Journal of Geophysical Research: Atmospheres*, *123*(16), 8538–8560. https://doi.org/10.1029/2018JD028714

Murphy, J. M., Garcia, S., Piston, A., Moss, J. H., Howard, K., Fergusson, E. A., et al. (2022). Coastal surveys in Alaska and their application to salmon run-size and harvest forecasts. *North Pacific Anadromous Fish Commission Technical Report(18)*.

Nash, D., Rutz, J. J., & Jacobs, A. (2024). Atmospheric rivers in southeast Alaska: Meteorological conditions associated with extreme precipitation. *Journal of Geophysical Research: Atmospheres*, *129*(4), e2023JD039294. https://doi.org/10.1029/2023JD039294

Neiman, P. J., Ralph, F. M., Wick, G. A., Kuo, Y.-H., Wee, T.-K., Ma, Z., et al. (2008). Diagnosis of an intense atmospheric river impacting the pacific northwest: Storm summary and offshore vertical structure observed with cosmic satellite retrievals. *Monthly Weather Review*, *136*(11), 4398–4420. https://doi.org/10.1175/2008MWR2550.1

Paily, P., Macagno, E., & Kennedy, J. (1974). Winter-regime surface heat loss from heated streams. research report. *US Office of Scientific and Technical Information*. Retrieved from https://www.osti.gov/biblio/7179276

Paul, J. N., Lawrence, J. S., F. Martin, R., Mimi, H., & Gary, A. W. (2011). Flooding in western Washington: The connection to atmospheric rivers. *Journal of Hydrometeorology*, *12*(6), 1337–1358. https://doi.org/10.1175/2011JHM1358.1

Prowse, T., Bonsal, B., Duguay, C., & Lacroix, M. (2007). River-Ice break-up/freeze-up: A review of climatic drivers, historical trends and future predictions. *Annals of Glaciology*, *46*, 443–451. https://doi.org/10.3189/172756407782871431

Prowse, T. D., & Beltaos, S. (2002). Climatic control of river-ice hydrology: A review. *Hydrological Processes*, *16*(4), 805–822. https://doi.org/10.1002/hyp.369

Ralph, F. M., Dettinger, M. D., Cairns, M. M., Galarneau, T. J., & Eylander, J. (2018). Defining "atmospheric river": How the glossary of meteorology helped resolve a debate. *Bulletin of the American Meteorological Society*, *99*(4), 837–839. Retrieved from https://doi.org/10.1175/BAMS-D-17-0157.1

Ralph, F. M., Neiman, P. J., Wick, G. A., Gutman, S. I., Dettinger, M. D., Cayan, D. R., & White, A. B. (2006). Flooding on California's Russian river: Role of atmospheric rivers. *Geophysical Research Letters*, *33*(13). https://doi.org/10.1029/2006GL026689

Rey, D., & Neuhauser, M. (2011). Wilcoxon-signed-rank test. In M. Lovric (Ed.), *International encyclopedia of statistical science* (pp. 1658–1659). Springer Berlin Heidelberg. https://doi.org/10.1007/978-3-642-04898-2_616

Saavedra, F., Cortés, G., Viale, M., Margulis, S., & McPhee, J. (2020). Atmospheric rivers contribution to the snow accumulation over the southern andes. *Frontiers in Earth Science*, *26*, 5–37. https://doi.org/10.3389/feart.2020.00261

Shapiro, S. S., & Wilk, M. B. (1965). An analysis of variance test for normality (complete samples). *Biometrika*, *52*(3–4), 591–611. https://doi.org/10.2307/2333709

Shen, H. T. (2010). Mathematical modeling of river ice processes. *Cold Regions Science and Technology*, *62*(1), 3–13. https://doi.org/10.1016/j.coldregions.2010.02.007

Thornton, M., Shrestha, R., Wei, Y., Thornton, P., Kao, S.-C., & Wilson, B. (2022). Daymet: Annual climate summaries on a 1-km grid for north America, version 4 r1 [Dataset]. *ORNL Distributed Active Archive Center*. https://doi.org/10.3334/ORNLDAAC/2130

Thornton, P. E., Shrestha, R., Thornton, M., Kao, S.-C., Wei, Y., & Wilson, B. E. (2021). Gridded daily weather data for north America with comprehensive uncertainty quantification. *Scientific Data*, *8*(1), 190. https://doi.org/10.1038/s41597-021-00973-0

Viale, M., Valenzuela, R., Garreaud, R. D., & Ralph, F. M. (2018). Impacts of atmospheric rivers on precipitation in southern south America. *Journal of Hydrometeorology*, *19*(10), 1671–1687. https://doi.org/10.1175/JHM-D-18-0006.1

Wang, Z., Ding, Q., Wu, R., Ballinger, T. J., Guan, B., Bozkurt, D., et al. (2024). Role of atmospheric rivers in shaping long term arctic moisture variability. *Nature Communications*, *15*(1), 5505. https://doi.org/10.1038/s41467-024-49857-y

Wille, J. D., Favier, V., Gorodetskaya, I. V., Agosta, C., Kittel, C., Beeman, J. C., et al. (2021). Antarctic atmospheric river climatology and precipitation impacts. *Journal of Geophysical Research: Atmospheres*, *126*(8), e2020JD033788. https://doi.org/10.1029/2020JD033788

Zhang, P., Chen, G., Ting, M., Ruby Leung, L., Guan, B., & Li, L. (2023). More frequent atmospheric rivers slow the seasonal recovery of arctic sea ice. *Nature Climate Change*, *13*(3), 266–273. https://doi.org/10.1038/s41558-023-01599-3

Zhu, Y., & Newell, R. E. (1998). A proposed algorithm for moisture fluxes from atmospheric rivers. *Monthly Weather Review*, *126*(3), 725–735. https://doi.org/10.1175/1520-0493(1998)126<0725:APAFMF>2.0.CO;2